Research Article | Vol. 6, No. 11 | 1 Nov 2016 | OPTICAL MATERIALS EXPRESS 3427

Optical Materials EXPRESS

Highly concentrated phenanthrenequinone–polymethylmethacrylate composite for thick reflection holograms recording at 532 nm

ULADZIMIR MAHILNY,[1] ALEXANDRA TROFIMOVA,[1] SERGEY NAZAROV,[1,2] ALEXEI TOLSTIK,[1] RAINER HEINTZMANN,[2,3] AND ELEN TOLSTIK[2,4,*]

[1]*Belarusian State University, Nezavisimosti av. 4, 220030 Minsk, Belarus*
[2]*Leibniz Institute of Photonic Technology, Albert-Einstein-Straße 9, 07745 Jena, Germany*
[3]*Institute of Physical Chemistry and Abbe Center of Photonics, Friedrich Schiller University of Jena, Lessingstr. 10, 07743 Jena, Germany*
[4]*Elenatolstik@googlemail.com*
[*]*Elen.tolstik@ipht-jena.de*

Abstract: The formation of stable phase reflection holograms in highly-concentrated phenanthrenequinone - polymethylmethacrylate (PQ-PMMA) layers with a thickness of about 100 μm at 532 nm recording wavelength has been investigated. In spite of the low absorbance of the photosensitive material at the long wave edge of the absorption spectrum, a refractive index modulation of $4.2 \cdot 10^{-4}$ close to the practically reachable limit was achieved during the optical recording. Quantitative investigation of thermal and light treatment of the recorded holograms has demonstrated a tenfold increase of the diffraction efficiency (up to 60%) without disturbing the angular selectivity profile.

OCIS codes: (090.0090) Holography; (050.7330) Volume gratings; (190.7070) Two-wave mixing.

References and links

1. A. V. Veniaminov and U. V. Mahilny, "Holographic polymer materials with diffusion development: principles arrangement, investigation, and applications," Opt. Spectrosc. **115**(6), 906–930 (2013).
2. A. Popov, I. Novikov, K. Lapushka, I. Zyuzin, Y. Ponosov, Y. Ashcheulov, and A. Veniaminov, "Spectrally selective holographic optical elements based on a thick polymer medium with diffusional amplification," J. Opt. A, Pure Appl. Opt. **2**(5), 494–499 (2000).
3. R.I. Billmers, E.J. Billmers, R. Burzynski, J.F. Weibel, L.H.I. Heverley, M.K. Casstevens, T.P. Curran, and V.M. Contarino, "Narrow-band holographic optical filter using thick efficient holographic gratings," Proc. SPIE **4659** Practical Holography XVI and Holographic Materials VIII, 156 (2002).
4. R. K. Kostuk, W. Maeda, C. H. Chen, I. Djordjevic, and B. Vasic, "Cascaded holographic polymer reflection grating filters for optical-code-division multiple-access applications," Appl. Opt. **44**(35), 7581–7586 (2005).
5. U.V. Mahilny, D.N. Marmysh, A.L. Tolstik, V. Matusevich, and R. Kowarschik, "Phase hologram formation in highly concentrated phenanthrenequinone–PMMA media," J. Opt. A: Pure Appl. Opt. **10**, 085302 (2008).
6. E. Tolstik, A. Winkler, V. Matusevich, R. Kowarschik, U. V. Mahilny, D. N. Marmysh, Yu. I. Matusevich, and L. P. Krul, "PMMA-PQ Photopolymers for Head-Up-Displays," IEEE Photonics Technol. Lett. **21**(10), 784–786 (2009).
7. U. V. Mahilny, D. N. Marmysh, A. L. Tolstik, V. Matusevich, and R. Kowarschik, "Holographic volume gratings in glassy polymeric material as coupling elements of planar lightguides," Proc. SPIE **6733**, 673324 (2007).
8. H. Akbari, I. Naydenova, L. Persechini, S. M. Garner, P. Cimo, and S. Martin, "Diffractive optical elements with a large angle of operation recorded in acrylamide based photopolymer on flexible substrates," Int. J. Polym. Sci. **2014**, 918285 (2014).
9. U. V. Mahilny, D. N. Marmysh, A. I. Stankevich, A. L. Tolstik, V. Matusevich, and R. Kowarschik, "Holographic volume gratings in a glass-like polymer material," Appl. Phys. B **82**(2), 299–302 (2006).
10. E. Tolstik, O. Romanov, V. Matusevich, A. Tolstik, and R. Kowarschik, "Formation of self-trapping waveguides in bulk PMMA media doped with Phenanthrenequinone," Opt. Express **22**(3), 3228–3233 (2014).
11. E. Tolstik, O. Kashin, V. Matusevich, and R. Kowarschik, "Broadening of the light self-trapping due to thermal defocusing in PQ-PMMA polymeric layers," Opt. Express **19**(3), 2739–2747 (2011).
12. S.H. Lin, M. Gruber, Y.N. Hsiao, and K.Y. Hsu, "Holographic data storage in low-shrinkage doped photopolymer," Adv. Inform. Optics and Photonics, **317** (2008).
13. S. H. Lin, Y.-N. Hsiao, and K. Y. Hsu, "Preparation and characterization of Irgacure 784 doped photopolymers for holographic data storage at 532 nm," J. Opt. A. **11**(2), 024012 (2009).

#272067 http://dx.doi.org/10.1364/OME.6.003427
Journal © 2016 Received 21 Jul 2016; revised 17 Sep 2016; accepted 17 Sep 2016; published 5 Oct 2016

Optical Materials EXPRESS

14. J. Wang, X. Sun, S. Luo, and Y. Jiang, "Study on the mechanism of dark enhancement in phenanthrenequinone-doped poly(methyl methacrylate) photopolymer for holographic recording," Opt. Commun. **283**(9), 1707–1710 (2010).
15. A. V. Trofimova, A. I. Stankevich, and V. V. Mogil'nyi, "Phenanthrenequinone–polymethylmethacrylate composite for polarization phase recording," J. Appl. Spectrosc. **76**(4), 585–591 (2009).
16. A. Kuboyama, F. Kobayashi, and S. Morokuma, "Studies of the π→π* absorption bands of 9,10-phenanthrenequinone," Bull. Chem. Soc. Jpn. **48**(7), 2145–2148 (1975).
17. D. M. Togashi and D. E. Nicodem, "Photophysical studies of 9,10-phenanthrenequinones," Spectrochim. Acta A Mol. Biomol. Spectrosc. **60**(13), 3205–3212 (2004).
18. H. Kogelnik, "Coupled wave theory for thick hologram gratings," Bell Syst. Tech. J. **48**(9), 2909–2947 (1969).
19. S. Monneret, P. Huguet-Chantôme, and F. Flory, "m-lines technique: prism coupling measurement and discussion of accuracy for homogeneous waveguides," J. Opt. A, Pure Appl. Opt. **2**(3), 188–195 (2000).
20. D. N. Marmysh, V. V. Mogilny, and E. A. Tolstik, "Transformation of holographic gratings in polymer layers containing phenanthrenequinone," Bull. Russ. Acad. Sci., Physics **70**(12), 2056–2060 (2006).
21. M. SeGall, D. Ott, I. Divliansky, and L. B. Glebov, "Effect of aberrations in a holographic system on reflecting volume Bragg gratings," Appl. Opt. **52**(32), 7826–7831 (2013).

1. Introduction

Holographic materials based on photosensitive phenanthrenequinone (PQ) are known and have been widely investigated [1]. Due to possibility of postexposition thermo-amplification of a recorded hologram, such materials are suitable for recording of effective phase reflection holograms [2–6]. The success of phase reflection holograms is connected to their high spectral selectivity along with moderate angular selectivity. This makes them useful as highly selective spectral elements (filters, mirrors and etc.) being easy to adjust and reliable to operate. For these applications holographic layers of considerable thickness (~1000 μm) containing of approximately 0.5 mol. % PQ have typically been used to provide appropriate diffraction efficiency and spectral selectivity. In certain cases (e.g. hologram head-up displays [6], coupling elements of light guides [7], holographic lenses [8]) phase holographic elements with a lower selectivity are preferable. Spectral and angular constraints are getting weaker as the hologram's thickness decreases. However, the widely used technique of thermal polymerization of the monomer (usually methylmethacrylate) with PQ dissolved in it limits the maximal PQ concentration in the holographic material due to the restricted solubility of PQ in the monomer. Thus under constant PQ concentration, a decrease of the layer thickness is connected with lowering of the holographic diffraction efficiency. In order to increase the PQ concentration to maintain the high value of the diffraction efficiency, another way of holographic layer preparation based on pouring of PQ and polymethylmethacrylate (PMMA) solution on a substrate and subsequent drying has been used in [9]. Such highly-concentrated PQ-PMMA layers with 100-200 μm thickness demonstrated the effective recording of transmission and reflection holograms [5, 9] as well as the formation of the waveguiding structures [10, 11] applying the radiation of argon laser (488 and 514.5 nm). At the same time it seems attractive to fabricate optical holographic elements by means of compact and powerful DPSS lasers at the wavelength of 532 nm. Laser radiation at 532 nm was repeatedly used for the recording of phase holograms in PQ-PMMA media under low concentration of PQ [12–14]. However increased PQ concentration causes strong intermolecular interactions between polar PQ molecules of specific (dimerization [15]) and probably universal types. In these circumstances the edge optical absorption can be formed by PQ molecules with photochemical properties (e.g. quantum efficiency of photoattachment to polymer matrix) nonoptimal for the holographic recording. Moreover, an inhomogeneous broadening of the absorption band due to sensitivity of its spectral position to a polarity of the environment [16] could possibly exclude a considerable part of photosensitive PQ molecules from the phototransformation process.

In this connection the objective of the present study was to determine the effectiveness of all stages of phase reflection hologram formation in highly-concentrated PQ-PMMA layers under recording by a DPSS laser at the wavelength of 532 nm.

Optical Materials EXPRESS

2. Material

Photosensitive layers of 100 ± 8 μm thickness were prepared by pouring the liquid solution of PMMA (120 000, Sigma-Aldrich) and PQ (Fluka) in chloroform on a glass substrate with subsequent drying at 60°C and then at 80°C. The content of PQ in the layer was 3 mol. %. The initial absorption spectrum of the polymer layer and its changes during irradiation are shown in Fig. 1.

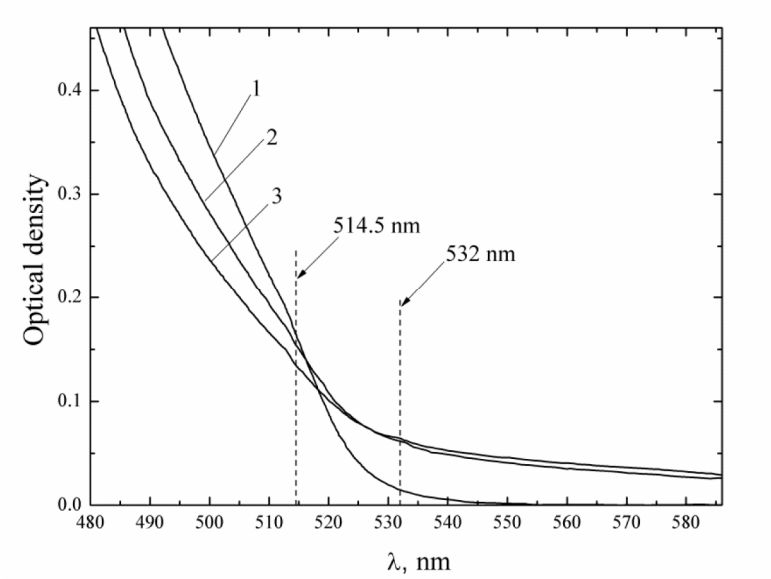

Fig. 1. Absorption spectrum of unexposed PQ-PMMA layer (1) of 100 μm thickness and spectra after uniform laser irradiation (λ = 532 nm) with exposure dose of 100 (2) and 200 (3) J·cm^{-2}.

The excitation of PQ molecules by 532 nm laser radiation occurs predominantly at the very edge of the $n\rightarrow\pi^*$ absorption band that is observed in the form of the bend on the wing of the absorption curve [17]. The laser line at 514.5 nm is situated much closer to $n\rightarrow\pi^*$ maximum (see Fig. 1). The optical density of the holographic layer at 514.5 nm is initially almost in one order higher compared to 532 nm.

As the exposure dose grows the spectrum changes (see Fig. 1, curves 2 and 3); short-wave absorption decreases and long-wave absorption increases. The latter is most likely the result of minor PQ photoproduct formation not allowing to estimate the PQ photoconversion from the absorption near 532 nm.

Figure 2 shows the principle scheme of photochemical conversion, including photoreduction of PQ followed by attachment of the primary photoproduct to the polymeric matrix [1].

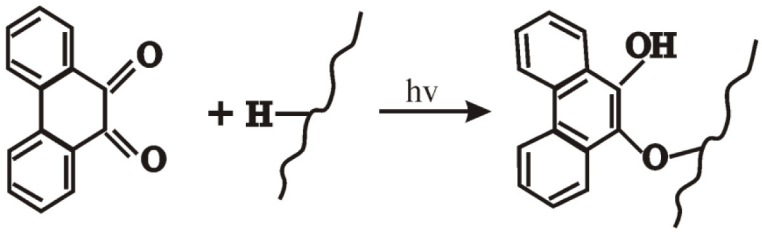

Fig. 2. Scheme of PQ photoproducts attachment to the polymer matrix.

Optical Materials EXPRESS

Being attached to macromolecules, the photoproducts become almost immobile, while the mobility of the PQ molecules, especially upon elevated temperatures, is quite enough to diffuse over about a full period of the recorded holographic grating. The diffusion leads to a homogeneous distribution of the PQ molecules and subsequently to the hologram amplification. Moreover, the intensified hologram becomes insensitive to the uniform activating irradiation in the visible spectral range and can be fixed by applying light. Consequently, three basic steps are required to form final hologram: optical recording, thermal treatment and light-induced fixation [1].

3. Experimental details

Volume phase reflection holograms were recorded using the Denisyuk scheme presented in Fig. 3, where the interfering field is formed by interference of the incident beam with the beam reflected from the mirror surface of the glass wedge (the beam ratio was 1:0.9). Recording was realized by 532 nm (30 mW) radiation of a DPSS laser, and the incident angle of activating light was changed by sample unit rotation (see Fig. 3). The polarization direction of the recording beams was set along the edge of the glass wedge. After the holographic recording the samples were thermally treated at different temperatures and then exposed homogeneously by polychromatic light of an LED lamp (LED-A60, ASD Corporation Limited, Hong Kong) with electrical power of 15 W and distance from the sample of 5 mm.

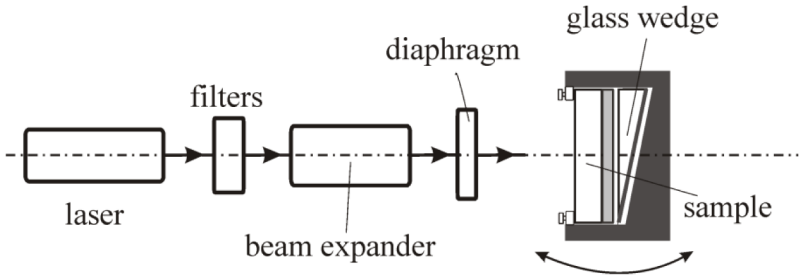

Fig. 3. Basic scheme of the hologram recording.

Following each stage of sample treatment the recording gratings were probed by laser radiation at λ = 532 nm and the measurements of the diffracted beams intensity was performed (see Fig. 4(a)).

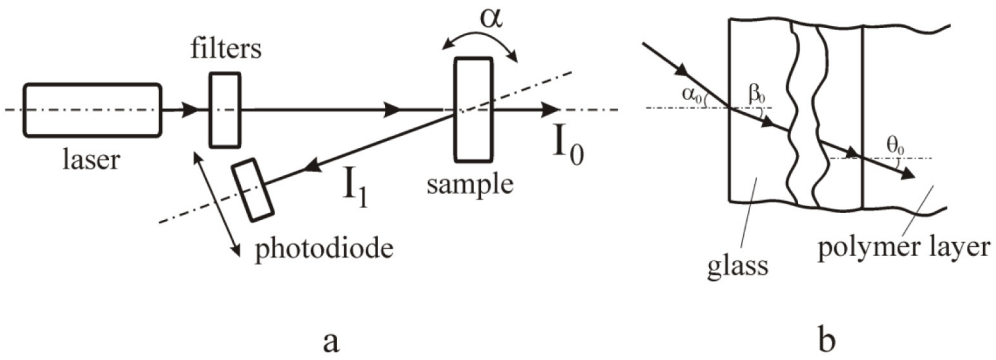

Fig. 4. The scheme of hologram's diffraction efficiency measurements (a) and optical path of probing beam in the sample (b).

The diffraction efficiency (η) was calculated as:

Optical Materials EXPRESS

$$\eta = \frac{I_1}{I_1 + I_0}, \tag{1}$$

where I_0 and I_1 are the intensities of 0-th and 1-st order diffracted beams. One should note that by calculating η as the ratio of the diffracted beam intensity to the input one, the value of η (for our experiments) decreases in less than 10% due to the influence of optical losses.

Using η values the modulation amplitude for the refractive index Δn was found from the following Equation [18]:

$$\Delta n = \frac{\lambda \cos(\theta_0)}{\pi l} arcth(\sqrt{\eta}), \tag{2}$$

where l is the layer thickness and θ_0 is the Bragg angle (measured in the medium). Being valid for an unslanted grating the formula (2) can be used also for the case of gratings recorded by the experimental scheme shown in Fig. 3 due to small value of wedge angle ε = 3° (the deviation did not exceed 0.1%).

Experimentally we defined the incidence angle α_0 (measured in the air) that related to θ_0 by Snell's law accordingly to Fig. 4(b):

$$\sin(\alpha_0) = n_g \sin(\beta_0) = n \sin(\theta_0) \tag{3}$$

where n_g is the refractive index of the glass (n_g = 1.52) and n is the average refractive index of the polymeric material (n = 1.51), obtained by commonly used m-lines technique [19].The angular characteristics of the recorded holograms were studied by measuring angular distributions of the diffracted light intensities (see Fig. 4) – their dependencies on values $\Delta\theta$ of a deviation from the Bragg angle. The value of angular selectivity ($\Delta\theta_{FWHM}$) was determined as a full width at half maximum of this distribution (FWHM).

4. Geometry of the reflection holographic gratings

Figure 5 presents the geometry of the recording scheme that was used. The reflection holographic grating is recorded by the interference pattern between two opposing collimated light beams: incident on the layer (reference beam) and reflected from the mirror back surface of the glass wedge (signal beam). As the mirror surface is oriented obliquely to the laser beam, the formed fringe pattern is slanted with respect to the medium boundaries at an angle $\gamma \neq 0$ with only very little dependence on α_0 of the incident recording beam (see Fig. 5) as demonstrated below.

Optical Materials EXPRESS

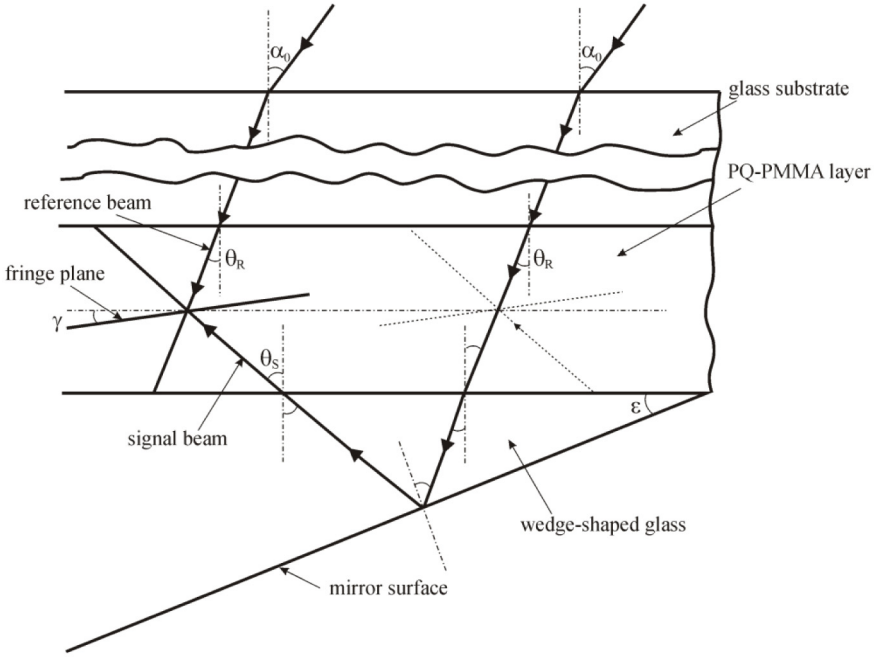

Fig. 5. Geometry of interfering beams formed in the scheme of holograms recording.

As shown in Fig. 5, using the geometry of Denisyuk scheme, the expression for the grating tilt angle γ can be obtained as:

$$\gamma = \frac{\theta_S - \theta_R}{2}, \tag{4}$$

where indices R and S correspond to the "reference" and "signal" waves forming the holographic grating.

The grating spacing d can be calculated from the Bragg condition:

$$2d\cos(\theta_R + \gamma) = \frac{\lambda_{rec}}{n}, \tag{5}$$

where λ_{rec} is the vacuum wavelength of the recording beam.

The values of d and γ, calculated by Eqs. (4) and (5) for different incident angles α_0 are given in the Table 1.

Table 1. Results of geometry analysis

α_0, grad	0	5	10	15
d, μm	0.176	0.177	0.179	0.181
γ, grad	3.020	3.020	3.020	3.021

The results show slight alteration of the grating period and constancy of the tilt angle with the changes of the angle of incidence. Both values are defined by the mutual orientation of the signal and reference beams (Eqs. (4) and (5)) and in the recording scheme of Fig. 5 these beams change their directions jointly while changing the angle of incidence of activating light.

Optical Materials EXPRESS

5. Reflection holographic gratings recording

For the recording of a volume reflection hologram in the PQ-PMMA material using the Denisyuk experimental set-up, an optimal exposure dose of layer irradiation was determined. To this aim the standard recording scheme of counter propagating beams was used and the intensity of diffraction in the course of the recording process was monitored, interrupting one of the beams for a short time. Figure 6 presents the kinetics of diffraction efficiency during the irradiation.

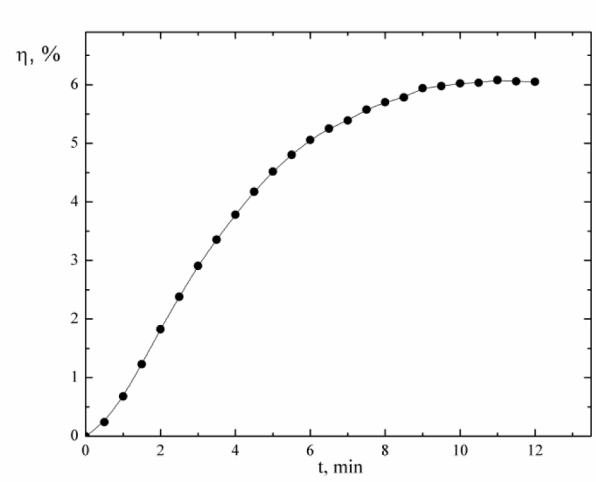

Fig. 6. The dependence of the grating diffraction efficiency on exposure time (light irradiance of 120 mW·cm^{-2}).

The diffraction efficiency follows a monotonic increase to a maximum value that is reached upon exposure doses of 85–90 J·cm^{-2}. Less exposure (≈10 J·cm^{-2}) is required for the effective holographic recording by applying a 514.5 nm laser [5], the difference can be explained by the different values of optical density at wavelengths of 532 nm and 514.5 nm (see Fig. 1).

Using estimated values of exposure dose, several reflection gratings have been recorded in the Denisyuk scheme at perpendicular incidence of laser beam on the layer surface. The maximal diffraction efficiency of the holograms directly after recording was ≈6%, which corresponds to a value of the modulation amplitude of the refractive index (Δn) of $4.2 \cdot 10^{-4}$ (according to the Eq. (2)). One can estimate a value of Δn by the Lorentz-Lorenz formula that with the assumption of complete PQ molecules addition to polymeric matrix gives the following expression [5]:

$$\Delta n = \frac{n^2 + 2}{6n} \Delta C_p \Delta R, \tag{6}$$

where ΔC_P is the modulation amplitude for the PQ photoproduct concentration, $\Delta R = R_P - R_{PQ}$, R_P and R_{PQ} are the molar refractions of photoproduct and PQ, respectively.

For the layer containing 3 mol.% of PQ, on condition that ΔC_P reaches 100% of the PQ concentration within the layer and using the estimated value of $\Delta R \approx 1.4$ cm^{3}mol^{-1} [5], the maximally reachable value of Δn can be estimated to $8.2 \cdot 10^{-4}$, almost twice the experimentally obtained value. This discrepancy may be a result of not being able to reach the 100% PQ consumption in the recording process. Besides, it is known that in the material under investigation, the value of Δn may decrease by 37% as a result of the nonsinusoidal profile of the transmission holographic grating [20]. Taking this into account one can

Optical Materials EXPRESS

conclude that the experimental value of $\Delta n = 4.2 \cdot 10^{-4}$ is fairly close to the theoretical estimation based on the data received under the holographic recording at 514.5 nm [5]. This result evidences for approximate invariance of the recording processes induced by 514.5 nm and 532 nm radiation.

6. Thermal amplification and light fixation

After recording, the holograms were thermally treated. Figure 7(a) shows the typical dependence of the diffraction efficiency on the time of post-exposure annealing at different temperatures.

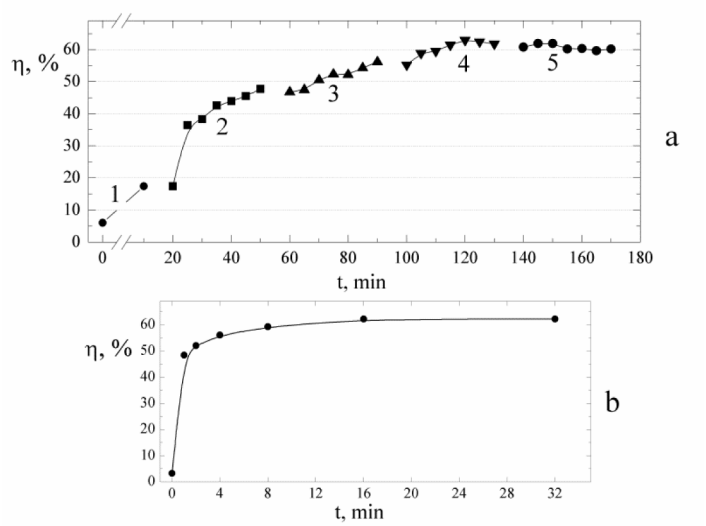

Fig. 7. Kinetics of diffraction efficiency changing upon stepwise heating: dark (at 20 °C) amplification in a day (1), at 50 (2), 60 (3), 70 (4) and 80 (5) °C (a) and continuous heating at 70 °C (b).

Each heating reveals an increase in η, gradually retarding at higher temperatures. The diffraction efficiency becomes unchangeable beginning from 70°C. As seen in Fig. 7(b), when heating is performed at constant temperature (70°C), a sharp growth of η is observed at the very beginning of the curve. Analysis of the experimental data presented in Fig. 7 allows us to select optimal values of heating temperature (70 °C) and its duration (≈20 min). In the optimal conditions of thermal treatment the modulation amplitude Δn increases by a factor of 4.3 ÷ 4.5. The values of amplification coefficient correspond to experimentally measured ones under holographic recording at 514.5 nm [5] to demonstrate of attachment extent preservation of PQ photoproducts to macromolecules under 532 nm excitation.

In the process of thermal treatment of the grating, a rather sudden change of the optimal incidence angle (α_0) of the probing beam corresponding to the Bragg angle (θ_0) was observed (instead of 0° α_0 becomes equal to ~6.5°). Later, upon sample cooling the angle returned to its initial value $\alpha_0 = 0°$ (as shown in Fig. 8).

Optical Materials EXPRESS

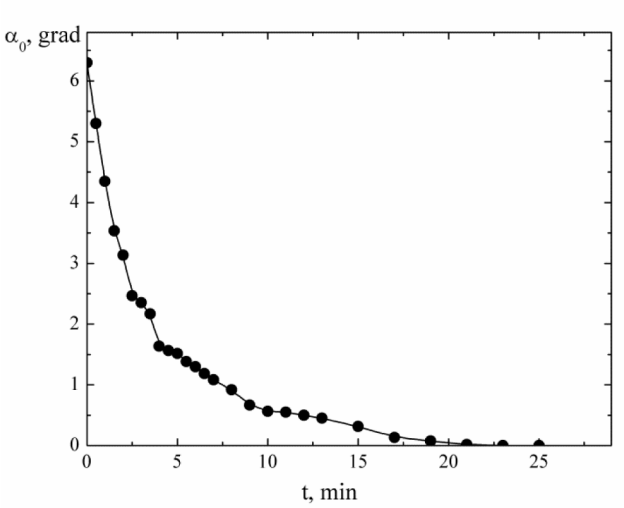

Fig. 8. The dark kinetics of incidence angle of probing beam corresponding to maximal diffraction efficiency in the course of hologram cooling.

The increase of α_0 (and of Bragg angle θ_0 correspondingly) under elevated temperature indicates an increase of the mean period of grating (<*d*>) due to thermal expansion of the polymer layer. The material shrinkage, taking place during the relaxation process, leads to the decrease of <*d*> down to the initial one. Hologram annealing may cause some inhomogeneity of the grating structure along the layer thickness after cooling. This, in turn, may lead to an unequal grating period as reflected in an asymmetrical shape of the angular selectivity curve [21]. The angular distribution of diffraction for the holographic grating recorded under $\alpha_0 = 0°$ after annealing was measured (see Fig. 9(a), dots). The maximum of the curve corresponds to the incidence angle of the recording beam (i.e. 0°) and no visible asymmetrical distortions of the curve were observed. From the data the value of $\Delta\theta_{FWHM} = 1.85°$ was calculated. The symmetry of selectivity curves was typical also for nonzero incidence angles of the recording laser beam (see Figs. 9(b)–9(d)). In addition we observed that the width of the angular curve decreased with the angle of incidence (value of $\Delta\theta$).

According to Kogelnik's coupled-wave theory [18], one can calculate the angular selectivity curve for volume hologram gratings. For reflection volume phase gratings with slanted fringes, the η of the grating is given by the following equations:

$$\eta = \left\{1 + \frac{1 - \xi^2 / \nu^2}{\sin h^2(\sqrt{\nu^2 - \xi^2})}\right\}^{-1} \tag{7}$$

$$\nu = \frac{i\pi\Delta n l}{\lambda_{prob}\sqrt{\cos(\theta)(\cos(\theta) - \frac{\lambda_{prob}}{nd}\cos(\gamma))}} \tag{8}$$

$$\xi = -\frac{\upsilon l}{2\left(\cos(\theta) - \frac{\lambda_{prob}}{nd}\cos(\gamma)\right)}, \tag{9}$$

where d is the grating spacing, λ_{prob} is the wavelength of the probing beam, l is the grating thickness, Δn is an amplitude of refractive index modulation, γ is the grating tilt angle, and θ

Optical Materials EXPRESS

is the incidence angle of the probing beam inside the material. The parameter υ accounts for $\Delta\theta$:

$$\upsilon = \Delta\theta \frac{2\pi}{d} \sin(\theta + \gamma), \tag{10}$$

Figure 9 (lines) shows the angular selectivity curves, calculated according to (7) – (10) for 100 μm thick gratings at various recording incidence angles α_0 (0°, 5°, 10° and 15°).

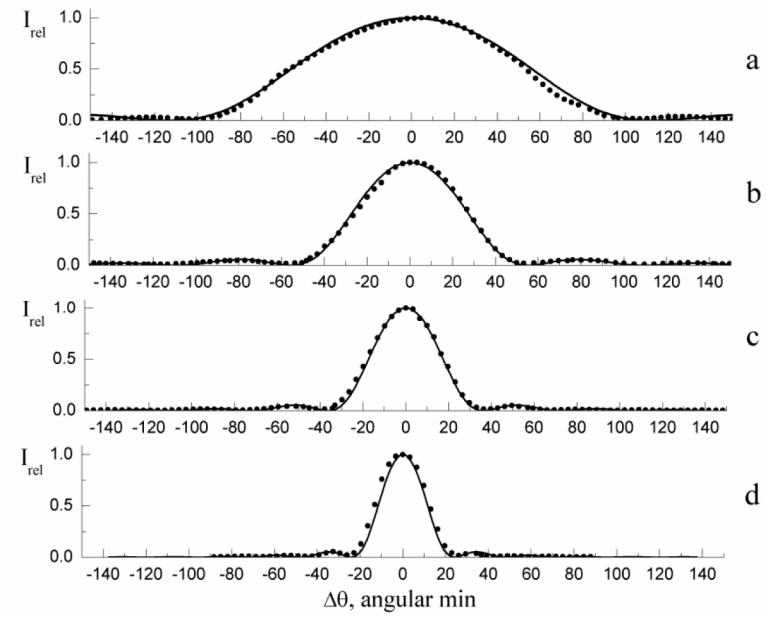

Fig. 9. Experimental (dots) and theoretical (lines) curves of angular selectivity of the gratings for different incidence angles of activating light: 0° (a), 5° (b), 10° (c) and 15° (d), normalized on the maximum diffraction efficiency value of ~60%.

As seen from Fig. 9, the calculated profiles correspond well to our experimentally measured angular dependences. Good correlation between the experimental data and Kogelnik's formulas confirmed that the recorded reflection gratings were homogeneous structures with a constant period along the thickness of the layer.

Thermal amplification of the recorded holograms is known to be the result of the diffusion of residual PQ molecules, whereas molecular photoproducts remain immobile being attached to polymeric matrix [1]. And under additional irradiation uniformly distributed photosensitive molecules create uniform distribution of their photoproducts. For permanent fixation of a holographic grating it is enough to expose it homogeneously after recording and annealing. Upon uniform irradiation the changes in the absorption spectrum continues as shown in Fig. 10 and the polymer layer gradually becomes almost completely transparent for visible long-wave region. It should be noticed that after light treatment no significant changes in the form and maximum position of angular selectivity curve (value of the Bragg angle) were observed.

Optical Materials EXPRESS

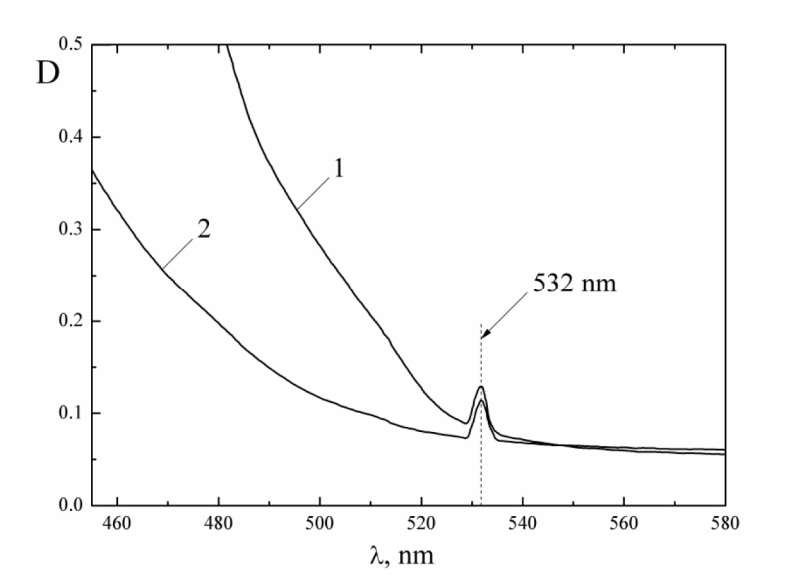

Fig. 10. Absorption spectra of PQ-PMMA thin layer with reflection grating before (1) and after (2) irradiation with LED lamp.

7. Summary

The investigations of the formation of volume phase reflection holograms in relatively thin PQ–PMMA layers at a high content of PQ, using the radiation of a 532 nm DPSS laser for the recording, are presented. The laser radiation is absorbed weakly at long wave edge of the absorption spectrum of photosensitive material, thus creating considerably different conditions compared to the recording at 514.5 nm. In the process of optical recording the refractive index modulation of $4.2 \cdot 10^{-4}$ was achieved. This was close to the practically achievable limit even though the absorption at 532 nm is rather low. Thermal (at 70 °C) and light treatments of the recorded holograms were quantitatively investigated resulting in a tenfold increase of the diffraction efficiency (up to 60%) without disturbing the angular selectivity profile. This confirmed the effectiveness of thermal amplification and homogeneity of the periodical holographic structures.

Funding

BMBF, project “3D Holmic” (01DK15011).